Stimulated Desorption by Surface Electron Standing Waves

M. T. Sieger,* G. K. Schenter, and T. M. Orlando
W. R. Wiley Environmental Molecular Sciences Laboratory, Pacific Northwest National Laboratory, P.O. Box 999, MSIN K8-88, Richland, Washington 99352
(Received 12 October 1998)

The total electron-stimulated desorption yield of Cl^+ ions from the Cl-terminated Si(111) surface is shown to exhibit fine-structure oscillations as a function of incident electron beam direction. We demonstrate that this fine structure is consistent with quantum-mechanical scattering and interference of the incident electron. Comparison of experimental data to a qualitative theory reveals the site of the excitation responsible for desorption, and the ground-state atomic bonding geometry of the desorbate. The data are consistent with desorption initiated by an excitation localized on the Si atom bonded to Cl. [S0031-9007(99)08922-X]

PACS numbers: 79.20.La, 61.14.Dc, 79.60.Dp

Materials modification by electron or photon beams and the desorption of surface-bound species induced by electronic transitions are phenomena of both technological and fundamental importance. The physics of desorption induced by electronic transitions, particularly electron-stimulated desorption (ESD) [1], is the basis for electron-beam induced processes in materials growth and etching, lithography, hot-electron induced defects in devices, radiation damage, and is important for other disciplines, including astrophysics [2]. Stimulated desorption is also a concern in many traditional surface probes such as photoemission, low energy electron diffraction (LEED), and electron microscopy since it results in damage. One issue central to understanding stimulated desorption is the relationship between the atomic and electronic structure of a surface species and its desorption probability. The majority of effort in experimental and theoretical ESD has focused on the mechanisms of desorption following excitation, of which the two most prominent are the Menzel-Gomer-Redhead and Knotek-Feibelman mechanisms [3,4]. These models have motivated the description of the desorption cross sections as the product of the excitation (inelastic electron-solid scattering) cross section and the total desorption or escape probability.

An aspect of stimulated desorption that has received much less attention is diffraction of the incident electron beam. Interference of the direct (or unscattered) electron wave with waves elastically scattered from the crystal lattice forms a "standing wave," with spatially localized maxima and minima in the incident electron density. Whether a particular site on a surface experiences a maximum or minimum depends on the wavelength (energy) of the electron, the direction of incidence relative to the crystal axes, and the arrangement of atoms in the lattice [see Fig. 1(a)]. Since the probability of desorption is proportional to the incident electron density at the site of the "absorber" (the site of the electronic excitation leading to desorption), the total ESD cross section should depend upon the local atomic structure and the **k** vector of the incident wave.

Electron diffraction has been previously observed to affect photon-stimulated desorption (PSD) measurements, through the extended x-ray absorption fine-structure effect [5,6]. These studies suggested that total ion yields could be used to gather structural information. However, further studies were not pursued since desorption induced by secondary electrons contributed significantly to the signal of interest [7]. Structural characterization of surfaces using stimulated desorption has therefore been limited to measurements of the ion desorption trajectories.

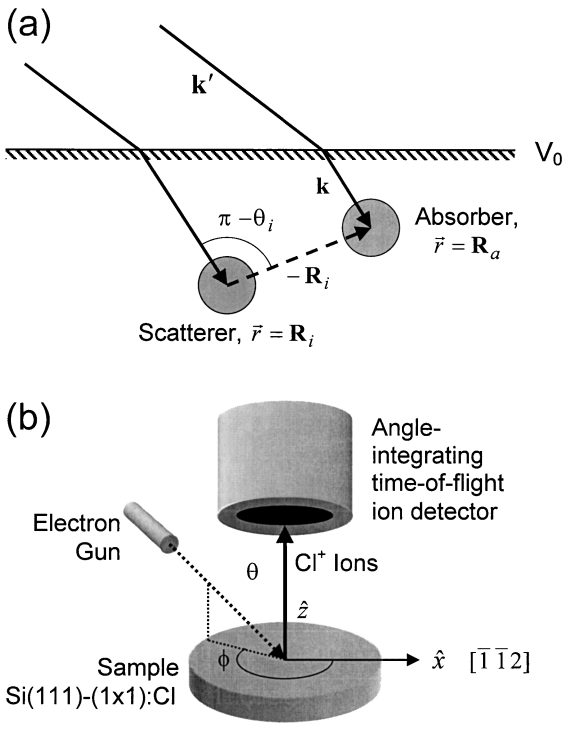

FIG. 1. (a) Illustration of the scattering geometry in the solid. The incident electron wave is denoted by $\mathbf{k}'$ and by $\mathbf{k}$ in the solid (corrected for the inner potential V_0). Scattering angles and vectors are described in the text. (b) Schematic diagram of the experimental apparatus (see text).

 0031-9007/99/82(16)/3348(4)$15.00

Electron-stimulated desorption ion angular distributions (ESDIAD) are related to the initial state bonding geometry because desorption trajectories typically follow bond axes [1,8]. While ESDIAD has been successful in measuring the bonding geometry of several adsorbate systems, it gives no direct information regarding bond distances. As a consequence, ESD has not been a widely utilized probe of surface structure, when compared to other surface spectroscopies.

In this Letter, we report experiments demonstrating, for the first time, that total ESD yields show fine structure as a function of incident electron direction and energy. This fine structure is consistent with scattering and interference of the incident electron to form a surface standing wave in the *initial state* of the desorption process. Comparison of experimental data to a qualitative model reveals the bonding geometry of the atomic site whose excitation is responsible for initiating the desorption process. Electron standing-wave stimulated desorption is potentially a powerful technique for surface structure determination, and for illuminating the relationship between localized states and excitations leading to desorption.

Our measurements were carried out in an ultrahigh-vacuum system (base pressure 2×10^{-10} torr) equipped with a rotating sample mount, a pulsed low energy (5–100 eV) electron gun, and a time-of-flight (TOF) mass spectrometer. Figure 1(b) is a schematic of the experimental geometry. We have chosen Cl-terminated Si(111) as a model system for this study, since the surface structure and electronic properties are well known [9–12]. The *n*-type Si(111) substrates were cleaned by heating to 1300 °C for 10 sec, then were cooled to 450 °C and exposed to 1×10^{-7} torr of Cl_2 for 1000 sec. Previous studies have shown that these preparation conditions yield a well-ordered (1×1) surface terminated by one monolayer of Cl atoms [13]. The sample was mounted such that the parallel component of the electron **k** vector pointed in the substrate $[\bar{1}\bar{1}2]$ direction (a mirror plane) at azimuth $\phi = 0°$. The electron gun has a fixed 45° polar angle of incidence relative to the sample normal. Data were acquired by leaving the electron gun and TOF spectrometer fixed, while the sample was rotated in azimuth. To ensure total ion collection, an extraction field pulse of -125 V was applied between the sample and the TOF entrance grid immediately following the electron pulse. The desorption rate was measured by integrating the area under the Cl^+ TOF peak. The electron energy threshold for producing Cl^+ ions was measured to be 17 eV. To minimize contributions to the fine structure from secondary electrons, data were acquired as close to the threshold as possible, in the range of 20–40 eV.

Figure 2 shows the total Cl^+ ion yield measured as a function of sample azimuth, at an electron energy of 25 eV. At the top of Fig. 2, the raw data (circles) are shown with a smooth fitted background curve I_0, modeling the desorption rate in the absence of incident beam diffraction. The

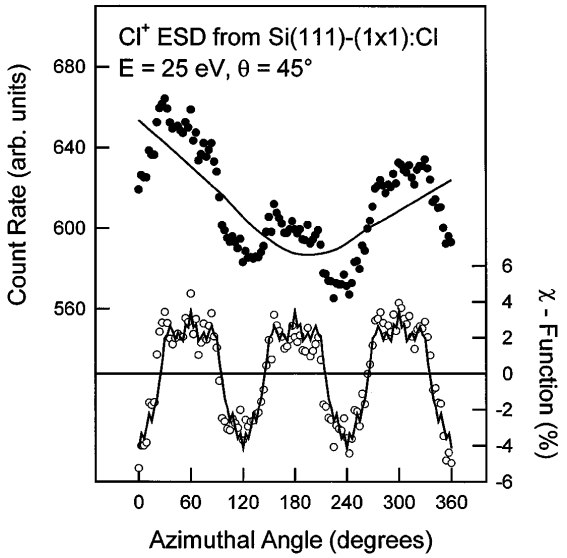

FIG. 2. The total Cl^+ ion yield measured as a function of sample azimuth ϕ, for a fixed polar angle of incidence $\theta = 45°$, and an electron energy of 25 eV. Top: Raw data (circles), with a smooth fitted I_0 curve (solid line). Bottom: Raw data (circles) and symmetry-averaged (solid line) χ function.

fitted I_0 curve is a weak function of azimuth, due to changes in the overall system detection sensitivity as the sample is rotated. The data are reproducible, with identical fine structure observed on several samples, and exhibit mirror planes in registry with those of the (111) substrate. The oscillatory part of the data $\chi = I/I_0 - 1$ characterizes the deviation from I_0 due to diffraction, and is shown in the lower part of Fig. 2. The raw χ function is then symmetry averaged. Care must be taken to prevent the introduction of spurious structure into the data when averaged in this manner. In our case, averaging introduced no structure which is not evident in the raw data. In Fig. 3(a) symmetry-averaged χ functions are plotted for data acquired at selected electron energies near threshold, along with calculations discussed below. Quantum-mechanical scattering and interference is expected to be a function of the electron energy, as observed. The peak-to-peak amplitude of χ is roughly 8% at 25 eV and *the angular structure contains information about the bonding geometry of the absorber.*

The measured χ functions can be subjected to structural analysis analogous to that used in angle-resolved photoelectron diffraction [14,15]. To demonstrate the structural origin of the observed fine structure, we have compared our data to a calculation assuming that the ESD rate is proportional to the probability of finding the incident electron in the vicinity of the absorber located at $\mathbf{R}_a$, or $I \propto \psi^*(\mathbf{R}_a)\psi(\mathbf{R}_a)$, where $\psi(\mathbf{r})$ is the incident electron wave function in the presence of the surface. In the absence of scattering, the electron wave function is $\psi^0(\mathbf{r}) = \exp(i\mathbf{k} \cdot \mathbf{r}) \exp[-z/\lambda \cos(\theta)]$, where **k** is the electron wave vector, corrected for refraction through the inner potential V_0

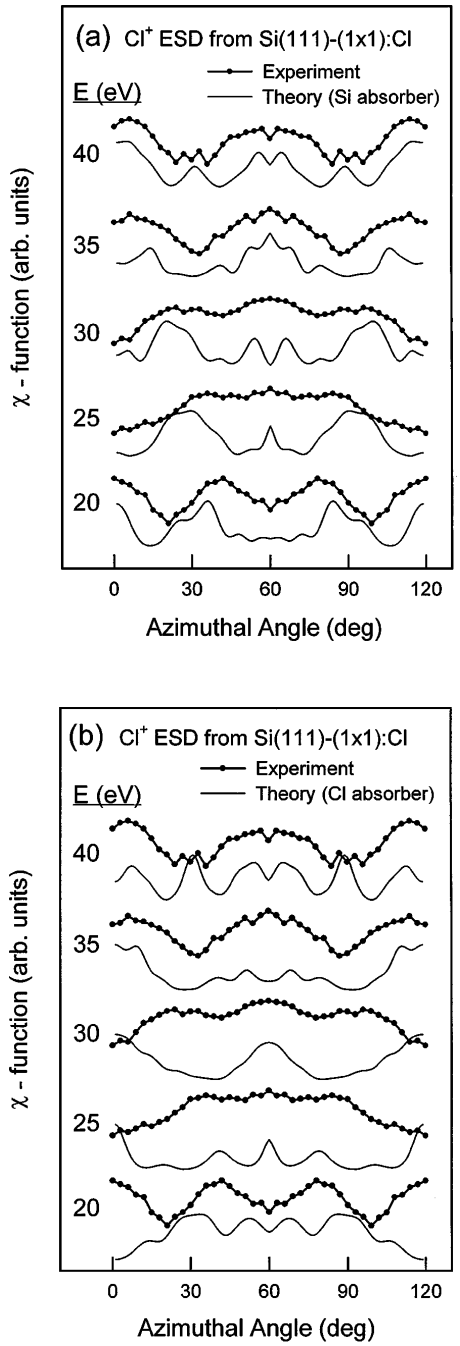

FIG. 3. Symmetry-averaged χ functions measured at several incident electron energies, with single-scattering cluster calculations obtained by Eq. (1). (a) Si absorber; (b) Cl absorber. The peak-to-peak amplitudes of the data and calculations have been normalized for display, with calculations offset for clarity.

[14]. The right-hand exponential represents attenuation of the incident plane wave from inelastic scattering processes, where the mean-free path is 2λ, z is the distance normal to the surface traveled in the solid, and θ is the angle between $\mathbf{k}$ and the surface normal. To first order in the scattering, the electron wave function in the presence of the surface can be approximated by

$$\psi(\mathbf{R}_a) \approx \psi^0(\mathbf{R}_a) + \sum_{i=1}^{N} \psi^0(\mathbf{R}_i) f_{\text{eff}} \frac{e^{ik|\mathbf{R}_i - \mathbf{R}_a|}}{k|\mathbf{R}_i - \mathbf{R}_a|} e^{-|\mathbf{R}_i - \mathbf{R}_a|/\lambda}, \quad (1)$$

where the $\mathbf{R}_i$ are bond vectors of the N lattice atoms in the cluster surrounding the absorber at $\mathbf{R}_a$. The curved-wave scattering factor f_{eff} is obtained using the separable-propagator method of Rehr and Albers [16] and reduces to the usual atomic scattering factor

$$f(\theta) = \sum_{\ell} (2\ell + 1) e^{i\delta_\ell} \sin(\delta_\ell) P_\ell(\cos(\theta)) \quad (2)$$

as $k|\mathbf{R}_i - \mathbf{R}_a| \to \infty$. The complex scattering phase shifts δ_ℓ were calculated using the FEFF 7.0 package developed by Rehr *et al.* [17]. Our model evokes several simplifying approximations: (1) only single-scattering terms are included, (2) the interaction with the absorber is assumed to occur at a point, (3) the absorber potential is ignored, and (4) the effect of lattice vibrations is neglected. While admittedly simplified, this model reproduces the essential features of the relevant physics. Calculations were performed with a 1028-atom ideal Cl-terminated Si(111)-(1×1) cluster (Cl-Si distance 2.03 Å [18]), containing all atoms within a 20 Å radius hemisphere of the absorber. The inner potential V_0 was fixed at 16 eV, and the inelastic mean-free path was chosen to be 5 Å.

A previous study of Cl^+ PSD from Si(111) assigned the excitation responsible for desorption to a Cl $3s$ to valence antibonding transition [11]. It was not possible to achieve a good match between calculation and experiment assuming that the excitation interaction is localized on the Cl atom. A very good match between theory and experiment was obtained, however, for excitation localized on the Si atom bonded to Cl. Figures 3(a) and 3(b) show symmetry-averaged data plotted with the results of calculations assuming Si and Cl absorbers, respectively. The qualitative agreement between the Si absorber model and data is very good. Since there is no density of states localized on Si at a binding energy of 17 eV (corresponding to the threshold energy), desorption does not appear to be initiated by a valence to antibonding, ionization, or Auger event. We therefore assign the excitation responsible for Cl^+ desorption to a shakeup or shakeoff event involving valence states localized on the Si atom. One or two holes are then transferred to the Cl, and reversal of the Madelung potential ejects the ion.

Having shown the existence of fine structure in ESD rates with incident beam direction and energy, established its origin in quantum-mechanical scattering and interference of the incident electron, and demonstrated the site selectivity of the data, we briefly discuss possible applications of this new technique. Beyond the applicability to determining the relationship between localized excitations and stimulated desorption, our method can contribute

to our understanding of other electron-surface probes, most notably Auger electron spectroscopy [15,19], where knowledge of incident beam diffraction (IBD) effects is necessary for the quantitative interpretation of data. Some studies have concluded that IBD is negligible compared to exit beam diffraction [20], while others maintain that IBD is important [19,21]. Since stimulated desorption does not suffer from detectable diffraction of the outgoing ion, it offers a way to measure incident beam diffraction independent of exit beam effects. Our data would suggest that standing-wave effects may cause variations in the Auger emission of up to 10% between different bonding sites.

While no one analysis technique can claim to determine unambiguous structural information in general, we believe this method has some unique features, and offers an intriguing complement to current techniques. Applications include systems not suitable for traditional probes such as LEED or photoelectron diffraction, such as radiation-sensitive materials. Since ESD is sensitive to surface minority sites, this technique may be applied to the structural characterization of dilute adsorbates and defects. Finally, stimulated desorption is not a passive technique, since material is actively removed from the surface during analysis. The data presented here demonstrate that, in principle, it is possible to choose the incident electron energy and direction to preferentially desorb atoms from specific surface bonding sites and affect a degree of control over electron-stimulated processes in materials growth and catalysis.

In conclusion, we have observed fine structure in the electron-stimulated desorption yield of Cl^+ ions from the Cl-terminated Si(111) surface with incident beam direction. This fine structure is consistent with scattering and interference of the incident electron wave in the initial state of the desorption process. Comparison of the data with a simple model reveals the excitation site to be localized on the Si atom bonded to Cl. Electron standing-wave stimulated desorption is potentially a useful technique for illuminating the relationship between atomic structure and stimulated desorption, and for surface structure determination.

The authors thank K. A. Briggman, D. P. Taylor, G. S. Herman, and W. C. Simpson for technical help. The research described in this paper was performed at the W. R. Wiley Environmental Molecular Sciences Laboratory, a national scientific user facility sponsored by the Department of Energy's Office of Biological and Environmental Research and located at Pacific Northwest National Laboratory. Pacific Northwest National Laboratory is operated for the U.S. Department of Energy by Battelle under Contract No. DE-AC06-76RLO 1830. This work is supported by the U.S. Department of Energy Office of Basic Energy Sciences, Chemical Sciences Division.

*Author to whom correspondence should be addressed. Electronic address: matt.sieger@pnl.gov

[1] For an extensive review of electron-stimulated desorption, see R. D. Ramsier and J. T. Yates, Jr., Surf. Sci. Rep. **12**, 3282 (1991), and references therein.
[2] For a discussion of the importance of desorption processes in astrophysics, see R. E. Johnson, *Energetic Charged Particle Interactions with Atmospheres and Surfaces* (Springer-Verlag, Berlin, 1990).
[3] D. Menzel and R. Gomer, J. Chem. Phys. **40**, 1164 (1964); **41**, 3311 (1964); P. A. Readhead, Can. J. Phys. **42**, 886 (1964).
[4] M. L. Knotek and P. J. Feibelman, Phys. Rev. Lett. **40**, 964 (1978).
[5] R. Jaeger, J. Feldhaus, H. Haase, J. Stohr, Z. Hussain, D. Menzel, and D. Norman, Phys. Rev. Lett. **45**, 1870 (1980).
[6] W. Drube, A. Lessmann, and G. Materlik, Rev. Sci. Instrum. **63**, 1138 (1992).
[7] R. Jaeger, J. Stohr, and T. Kendelewicz, Surf. Sci. **134**, 547 (1983).
[8] J. J. Czyzewski, T. E. Madey, and J. T. Yates, Jr., Phys. Rev. Lett. **32**, 777 (1974); T. E. Madey, Science **234**, 316 (1986).
[9] J. S. Villarrubia and J. J. Boland, Phys. Rev. Lett. **63**, 306 (1989); C. Yan, J. A. Jensen, and A. C. Kummel, Phys. Rev. Lett. **72**, 4017 (1994).
[10] G. Thornton, P. L. Wincott, R. McGrath, I. T. McGovern, F. M. Quinn, D. Norman, and D. D. Vvedensky, Surf. Sci. **211/212**, 959 (1989).
[11] T. D. Durbin, W. C. Simpson, V. Chakarian, D. K. Shuh, P. R. Varekamp, C. W. Lo, and J. A. Yarmoff, Surf. Sci. **316**, 257 (1994).
[12] R. D. Schnell, D. Rieger, A. Bogen, F. J. Himpsel, K. Wandelt, and W. Steinmann, Phys. Rev. B **32**, 8057 (1985); L. J. Whitman, S. A. Joyce, J. A. Yarmoff, F. R. McFeely, and L. J. Terminello, Surf. Sci. **232**, 297 (1990).
[13] J. J. Boland and J. S. Villarrubia, Phys. Rev. B **41**, 9865 (1990).
[14] For a review of photoelectron diffraction techniques, see C. S. Fadley, in *Synchrotron Radiation Research: Advances in Surface and Interface Science*, edited by Robert Z. Bachrach, Techniques Vol. 1 (Plenum Press, New York, 1992).
[15] S. A. Chambers, Surf. Sci. Rep. **16**, 261 (1992).
[16] J. J. Rehr and R. C. Albers, Phys. Rev. B **41**, 8139 (1990).
[17] S. I. Zabinsky, J. J. Rehr, A. Ankudinov, R. C. Albers, and M. J. Eller, Phys. Rev. B **52**, 2995 (1995); A. L. Ankudinov, S. I. Zabinsky, and J. J. Rehr, Comput. Phys. Commun. **98**, 359 (1996).
[18] P. H. Citrin, J. E. Rowe, and P. Eisenberger, Phys. Rev. B **28**, 2299 (1983).
[19] Y. Gao and J. Cao, Phys. Rev. B **43**, 9692 (1991); Y. U. Idzerda and G. A. Prinz, Phys. Rev. B **43**, 11 460 (1991).
[20] M. De Crescenzi, R. Gunnella, R. Bernardini, M. De Marco, and I. Davoli, Phys. Rev. B **52**, 1806 (1995); S. A. Chambers, I. M. Vitomirov, and J. H. Weaver, Phys. Rev. B **36**, 3007 (1987); S. A. Chambers, H. W. Chen, S. B. Anderson, and J. H. Weaver, Phys. Rev. B **34**, 3055 (1986).
[21] M. V. Gomoyunova, S. L. Dudarev, and I. I. Pronin, Surf. Sci. **235**, 156 (1990).